Autler-Townes effect in a sodium molecular-ladder scheme

Ruth Garcia-Fernandez, Aigars Ekers, Janis Klavins,* Leonid P. Yatsenko,† Nikolai N. Bezuglov,‡ Bruce W. Shore,§ and Klaas Bergmann

Department of Physics, University of Kaiserslautern, Erwin-Schrödinger Strasse, D-67663 Kaiserslautern, Germany

(Received 1 October 2004; published 1 February 2005)

We report results from studies of the Autler-Townes (AT) effect observed in sodium molecules from a molecular beam. A relatively weak laser field P couples an initially populated rovibronic level g in the electronic ground state (here $X\,^1\Sigma_g^+, v''=0,\ J''=7$) to a selected excited rovibronic level e (here $A\,^1\Sigma_u^+, v'=10,\ J'=8$), which in turn is coupled by a relatively strong laser field S to a more highly excited level f (here $5\,^1\Sigma_g^+, v=10,\ J=9$), a scheme we idealize as a three-state ladder. The AT effect is seen by scanning the frequency of the P field while recording fluorescence from both the e and f levels in separate detection channels. We present qualitative theoretical considerations showing that, when the P field is weak, the ratio of doublet component areas in the excitation spectrum from level f can be used to determine the lifetime of this level. We obtain a value of 17 ± 3 ns. When the P field is stronger, such that its Rabi frequency is larger than the decay rate of level e, the fraction of f-level population that decays to the intermediate electronic state $A\,^1\Sigma_u^+$ can be deduced from the AT spectrum. When supplemented with values of Franck-Condon and Hönl-London factors, our measurements give a value for the branching ratio (the fraction returning to level e) of $r_e=0.145$ with a statistical error of ±0.004. The use of a strong P field on the g-e transition and a weak S field as a probe on the e-f transition results in complex line shapes in the excitation spectrum of level f, not showing the familiar Autler-Townes doublet structure.

DOI: 10.1103/PhysRevA.71.023401 PACS number(s): 42.50.Hz, 33.80.−b, 33.40.+f, 33.70.Ca

I. INTRODUCTION

A common use of laser-induced excitation is to determine, by observation of fluorescence, the electronic and rovibrational structure of molecules [1]. Such fluorescence signals, plotted as a function of the probe laser frequency, typically reveal absorption-line profiles that are convolutions of molecular rest-frame profiles (characterized by homogeneous widths due to loss from spontaneous emission, predissociation, and collisions) with Doppler shifts that introduce inhomogeneous contributions to the widths.

When the excited state e is also near-resonantly coupled to a third state f by a second, strong laser field through an allowed electric-dipole transition, then the excitation signal becomes significantly modified; for a sufficiently strong *coherent* field, it appears as two distinct components, a pattern often termed the Autler-Townes (AT) doublet, honoring those who first observed it [2]. The AT effect originates with an energy shift produced by a resonant or near-resonant oscillating electric field, in contrast to the dynamic (or ac) Stark effect [3], which is produced by a nonresonant field (and which therefore varies quadratically rather than linearly with the electric field strength).

The AT effect has been extensively studied in atoms (for representative publications see [4]) and numerous papers have presented its theory in detail [5]. In molecules the optical AT effect has been much less studied; see for example [6].

The frequency separation of the two AT components provides a measure of the stronger-field interaction energy (Rabi frequency times $\hbar$), which is the product of a dipole transition moment of the atom or molecule and the electric field amplitude of the strong laser [7]. Thus it offers a technique for measuring dipole transition moments [8]. The present work provides an overview of results from a variety of experimental scenarios together with a mostly qualitative discussion. In particular, we show that the AT effect can be used to determine the ratio of lifetimes of the two strongly coupled levels and branching ratios of decay from the upper excited molecular states. A more detailed theoretical analysis of some of the observed spectra will be presented in a future publication [9].

II. THE LADDER COUPLING SCHEME

We consider specifically a ladderlike level scheme appropriate to sodium molecules. The three levels of interest, labeled g, e, and f, are ordered by increasing energy $E_g<E_e<E_f$. They bear the following electronic, vibrational and rotational labels in the present work:

*Permanent address: Institute of Atomic Physics and Spectroscopy, University of Latvia, Raina bulv. 19, LV-1586 Riga, Latvia.

†Permanent address: Institute of Physics, Ukrainian Academy of Sciences, prospect Nauki 46, Kiev-39, 03650, Ukraine.

‡Permanent address: St. Petersburg State University, Fock Institute of Physics, Petrodvorets, Ulianovskaya ul. 1, 198904 St. Petersburg, Russia.

§Permanent address: 618 Escondido Cir., Livermore, CA 94550, USA.

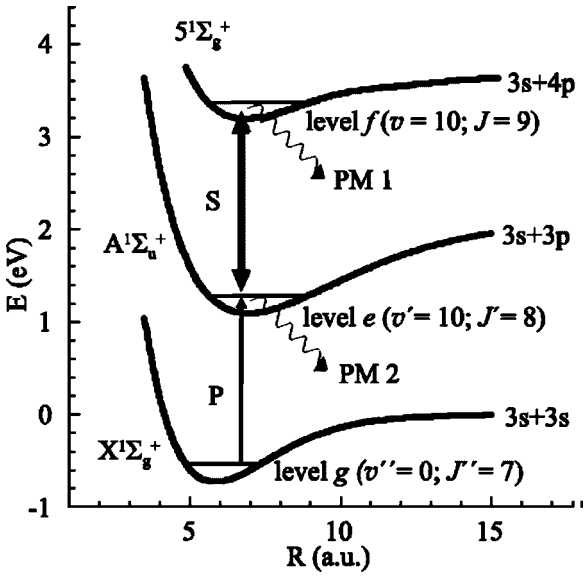

FIG. 1. Ladder level scheme in Na_2. The strong S field couples the $v'=10, J'=8$ level in the $A\,^1\Sigma_u^+$ state with the $v=10, J=9$ level in the $5\,^1\Sigma_g^+$ state. The weak probe field P is scanned across the resonance with the $X\,^1\Sigma_g^+, v''=0, J''=7 \rightarrow A\,^1\Sigma_u^+, v'=10, J'=8$ transition. The fluorescence from the $A\,^1\Sigma_u^+$ and $5\,^1\Sigma_g^+$ states is registered separately in two detection channels, termed PM1 and PM2.

$$\text{level} \quad g: \quad X\,^1\Sigma_g^+, \quad v''=0, J''=7,$$

$$\text{level} \quad e: \quad A\,^1\Sigma_u^+, \quad v'=10, J'=8,$$

$$\text{level} \quad f: \quad 5\,^1\Sigma_g^+, v=10, \; J=9.$$

The population initially resides in level g, the ground level of the ladder. Level e has a radiative lifetime of 12.45 ns [10], corresponding to a homogeneous linewidth of 12.78 MHz. The lifetime of level f has not been reported previously; measurements reported here lead to a value of 17 ± 3 ns.

Figure 1 shows the levels of interest and the radiative couplings that form a three-level ladder. The excited levels e and f are linked (resonantly or near-resonantly) by an allowed dipole transition induced by a relatively strong coherent field, here termed the strong field S (elsewhere called the dressing field or pump field), having a wavelength of 587 nm. The ground level g is linked to level e via electric-dipole transition induced by a weaker field, here called the probe field P, of wavelength 633 nm.

We shall here regard the excitation of this three-level ladder as modeled by three nondegenerate quantum states whose evolution is governed by the time-dependent Schrödinger equation subject to population loss. (By population we mean the probability of finding a molecule in a specific state at a particular time.) Because of angular momentum degeneracy (for angular momentum quantum number J there are $2J+1$ degenerate sublevels, each identified with a magnetic quantum number M), the molecular system of interest is not exactly three linked quantum states, as we idealize it. However, reasoning presented in Sec. V A provides justification for the three-state approximation.

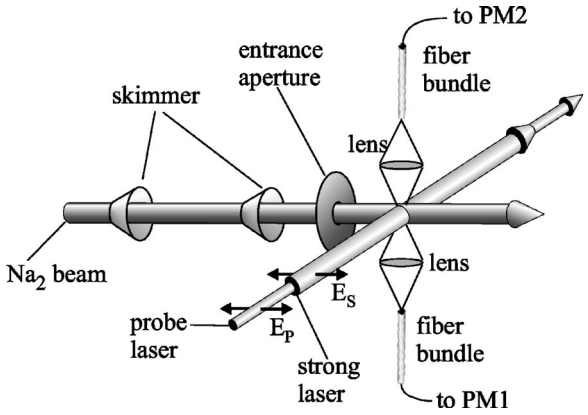

FIG. 2. Schematic layout of the molecular beam, laser beams, and detectors, showing skimmers, entrance aperture, and laser polarization direction. In reality, the laser beams are elongated in the vertical direction.

III. THE EXPERIMENT

The experiments were performed in a supersonic beam of Na_2 molecules, which crosses two parallel laser beams (see Fig. 2). The supersonic expansion cools the molecules so that 99% of them are in the ground vibrational level $v''=0$, while the distribution over the rotational levels peaks at $J''_{max}=7$. In the zone where the two laser fields interact with the molecules, the number density of molecules is about 2×10^{10} cm^{-3}. The flow velocity of the molecules in the beam is $v_f=1340$ m/s, and the full $1/e$ width of the longitudinal velocity distribution is $\Delta v_{mol}=260$ m/s. Two skimmers and an entrance aperture of the excitation zone collimate the beam to a divergence angle of $0.73° \pm 0.02°$, corresponding to a residual velocity spread of ± 8.5 m/s in the direction perpendicular to the beam axis. This corresponds to an inhomogeneous Doppler width [full width at half maximum (FWHM)] of 27 MHz for the P laser and 29 MHz for the S laser.

The molecular beam axis crosses the axes of two copropagating cw laser beams (both Coherent Co., CR-699-21 dye lasers, with linewidth $\Delta \nu_L = 1$ MHz) at right angles (see Fig. 2). The laser beams are focused by cylindrical lenses, with the long axis (the height) oriented perpendicular to the molecular beam axis. Both laser beams have the same linear polarization, which is held parallel to the molecular beam axis.

The two laser beams provide the P and S fields of Fig. 1. The frequency ω_P of the (weaker) first-stage P laser, with a power of typically $\leqslant 0.1$ mW, is scanned through resonance with the g-e transition $X\,^1\Sigma_g^+, v''=0, J''=7 \rightarrow A\,^1\Sigma_u^+, v'=10, J'=8$. The (stronger) second-stage S laser, of frequency ω_S and with a power of typically a few hundreds of milliwatts, is tuned near resonance with the e-f transition $A\,^1\Sigma_u^+, v'=10, J'=8 \rightarrow 5\,^1\Sigma_g^+, v=10, J=9$.

The positions and focus dimensions of both beams are monitored by means of a beam-profile measurement device (Dataray Beamscope-P7) having 5.0-μm-wide slits. The axes of the two laser beams coincide, but the S-laser beam is focused to a Gaussian waist of 160 μm diameter (FWHM),

which is more than three times larger than the 50 μm waist of the *P*-laser beam. With such adjustment, the *S* field can be considered as constant, and maximal, across the entire profile of the *P* field. The transit time (fly-through time [11]) of the molecules across the *P*-laser profile is 37 ns. The beam heights are 5.0 and 7.5 mm FWHM, for the *P* and *S* beams, respectively, corresponding to effective areas of 0.28 and 1.36 mm^2.

The fluorescence of the excited molecules is collected by lenses and imaged into two optical fiber bundles. The latter are positioned at opposite sides of and at right angles to the axes of molecular and laser beams (see Fig. 2). The light passes from the fibers, through spectral filters, into photomultipliers PM1 and PM2.

The detector PM1 is equipped with a cutoff filter that does not transmit light with wavelengths longer than 600 nm. This detector registers the fluorescence from level *f* to rovibronic levels of the electronic state $A\,^1\Sigma_u^+$ (including level *e*). The Franck-Condon factors for these transitions are such that the probability of spontaneous transitions from level *f* is appreciable only for the vibrational levels $v'=8-12$ of the $A\,^1\Sigma_u^+$ electronic state around the level *e* [12]. In fact, about 94% of the population that reaches the $A\,^1\Sigma_u^+$ electronic state from level *f* returns to the $v'=10$ level [12]. We refer to the signal from PM1 as the *f*-level fluorescence.

The detector PM2 accepts only light with wavelengths longer than 620 nm. It registers the fluorescence from all populated levels in the $A\,^1\Sigma_u^+$ electronic state (including the level *e* directly excited by laser radiation) and the levels populated by spontaneous decay of level *f* of the $5\,^1\Sigma_g^+$ electronic state. We refer to the signal from PM2 as the *e*-level fluorescence.

IV. SPECTRA

The excitation spectra were obtained by fixing the frequency of the *S* laser and sweeping the frequency of the *P* laser through resonance with the *g*-*e* transition, while monitoring simultaneously but separately the fluorescence from the levels *e* and *f*. We present these data as a function of the *P*-field detuning Δ_P for fixed *S*-field detuning Δ_S, where

$$\Delta_P \equiv \omega_P - (E_e - E_g)/\hbar, \quad \Delta_S \equiv \omega_S - (E_f - E_e)/\hbar.$$

Note that an increase in either laser frequency accompanies an increase in detuning.

The wavelengths of the light emitted by the *S* and *P* lasers are measured to an accuracy of ±0.001 nm using a wavemeter (Burleigh WA20). The zero of the *S*-field detuning was assigned to the frequency for which the AT splitting is smallest (cf. Sec. V C), as determined by interpolating measurements taken for a set of different *S*-field frequencies. The zero of the *P*-field detuning was assigned to the frequency which maximized the fluorescence output from the *e* level when the *S* field was blocked.

As will be discussed in Sec. V C, each of the two peaks appearing in the spectra (the AT doublet) can be attributed to a transition induced by the *P* field between the ground state ψ_g and one of two adiabatic states Φ_1 or Φ_2 constructed as superpositions of states ψ_e and ψ_f, with a relative composition that depends on the strength of the *S* field as parametrized by a mixing angle θ. By definition, adiabatic state Φ_2 has the higher energy [see Eq. (4b) below]; it appears as the right-hand peak (positive *P*-field detuning) in each of the figures.

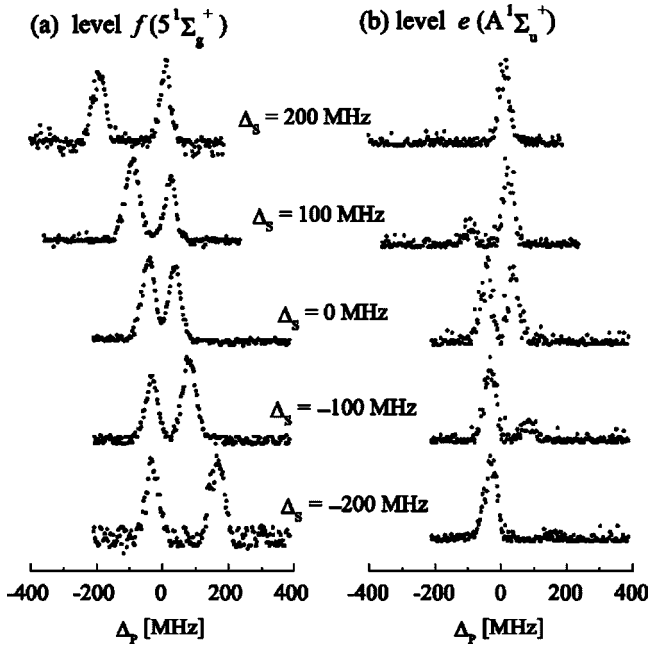

FIG. 3. Fluorescence signals (a) from level $f(5\,^1\Sigma_g^+)$ and (b) from level $e(A\,^1\Sigma_u^+)$ as a function of the *P*-field detuning Δ_P from resonance with the *g*-*e* transition, for five values of the detuning Δ_S of the *S* field from resonance with the *e*-*f* transition between +200 and −200 MHz. The *S*- and *P*-laser powers are 300 mW and 75 μW, respectively; the *P*-field Rabi frequency is 4.3 MHz.

Inevitably our two lasers undergo short-time fluctuations in phase and frequency, observable as the finite bandwidth. In addition, the lasers may drift in frequency or intensity during the 3 min required to record an excitation spectrum. Such effects can distort the AT profiles, causing unequal widths and/or unequal peak heights. From the statistics of the recorded spectra we estimate that such effects can cause variability in width of 6 MHz and variability of height ratios of ±10%.

Because some of the population from level *f* decays spontaneously to level *e*, some features of the *f*-level spectra are carried over to the *e*-level fluorescence, thereby altering the "clean" *e*-level signal predicted by theory. Furthermore, the signal detected by PM2 includes fluorescence from other levels of the $A\,^1\Sigma_u^+$ electronic state that are populated by decay of level *f*. By comparing the spectra of Figs. 3(a) and 3(b) for large and small detunings of the *S* field ($|\Delta_S| > 220$ MHz) we estimate that this contribution to the *e*-level fluorescence, when the *P* field is weak, is smaller than 10%.

A. Characterizing field strengths

The qualitative characteristics of the AT spectra from both levels *e* and *f* differ according to the intensity of the *P* field, I_P. It is useful to characterize the strength of this field by its

associated Rabi frequency Ω_P, and to refer to it as weak, intermediate, or strong by comparing this with various other frequencies or inverse times. (Note: all formulas involving frequencies are for angular frequencies, rad/s, although numerical values are given in hertz.)

One characteristic time scale is the pulse duration τ_{pulse}, from which one obtains the Fourier limit to the bandwidth from $1/\tau_{pulse}$. The pulse duration for our experiment, evaluated from the transit time of the molecules across the profiles of the laser beams, gives a bandwidth of 4 MHz.

An important time scale is the radiative lifetime of the excited level, τ_e. From $\gamma_e \equiv 1/\tau_e$ one obtains, for the present experiment, a frequency of about 13 MHz. This parameter provides a useful limit on what can be considered a "weak" field: one for which the Rabi frequency is less than the radiative rate, $\Omega_P < \gamma_e$.

Between these two limits lies the characteristic frequency associated with optical pumping, $1/\sqrt{\tau_{pulse}\tau_e}$. The relevance of this parameter derives from depletion of population from the ground state, a time-integrated effect associated with saturation of the transition, as characterized by the saturation parameter for an open system [13]

$$(\Omega_P)^2 \ \tau_{pulse}\tau_e = I_P/I_{sat}. \tag{1}$$

Typically one refers to a "saturating" field as one for which this saturation parameter exceeds unity; this is equivalent to the requirement that the Rabi frequency exceed the optical pumping rate, $\Omega_P > 1/\sqrt{\tau_{pulse}\tau_e}$. The saturation intensity I_{sat} for this transition is 65 mW/cm^2. For our laser-beam geometry this corresponds to a saturation power 0.16 mW. In calculating this we have used the electronic dipole moment $d_{ge}^{elec} = 9.14$ D [14], the Franck-Condon (FC) factor $S_{FC} = 0.095$ [15], and the Hönl-London (HL) factor $S_{HL} = 8/17$ to produce the needed total dipole moment $d_{ge} = d_{ge}^{elec}\sqrt{S_{FC}}\sqrt{S_{HL}} = 1.93$ D.

Yet another relevant frequency is the Doppler width for the *P*-laser wavelength, which here is 27 MHz. This parameter quantifies the range of detunings that contribute to any given excitation spectra and thereby establishes a limit to the resolution of structure in the spectra.

We term the *P* field to be "strong" when it produces a Rabi frequency Ω_P comparable to that of the *S* field, Ω_S. In this regime the *P* field can no longer be considered as a probe field. We term the *P* field to be "intermediate" when $\gamma_e < \Omega_P$ and yet $\Omega_P \ll \Omega_S$.

B. Weak *P* field and strong *S* field

Figure 3 shows the excitation spectra for five choices of the *S*-field detuning, for the case of weak (unsaturated) *P*-field intensity. For these and all other spectra the data of each scan were normalized to give unit height for the largest feature. Quantitative analysis of these displays is only possible within a single scan, i.e., for measurements of widths or ratios of peak heights.

The observations fit the typical pattern of a well-resolved Autler-Townes doublet. The separation between the doublet components is smallest when the *S*-field detuning Δ_S is zero; then it is equal to the Rabi frequency (see Sec. V C). By

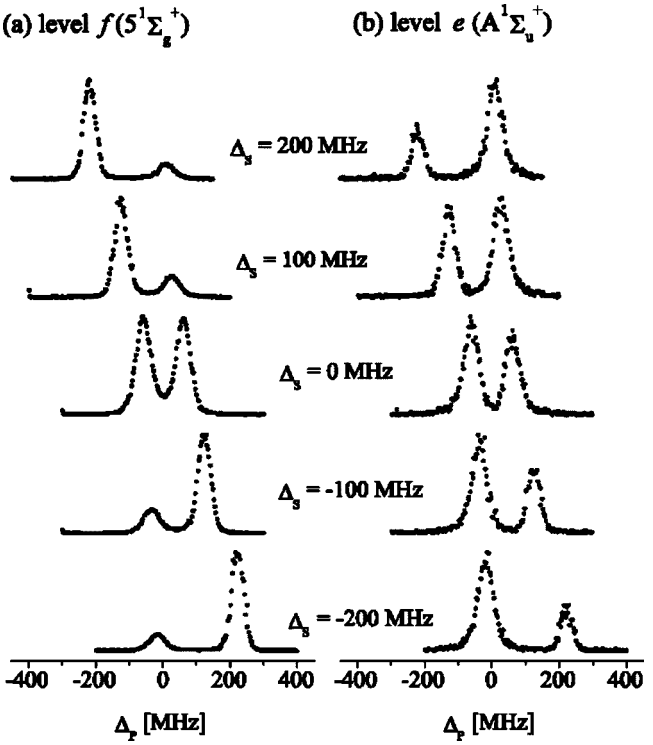

FIG. 4. As in Fig. 3 but with *S*- and *P*-laser powers of 590 and 2.4 mW, respectively; the *P*-field Rabi frequency is 25 MHz.

fitting the measured splittings to a function of detuning we determined the Rabi frequency associated with the *S* field and the *e*-*f* transition. For Fig. 3(a) (level-*f* spectra) it is 72 ± 6 MHz, while for Fig. 3(b) (level-*e* spectra) it is 79 ± 6 MHz. Elementary theory predicts that both spectra should exhibit the same Rabi frequency, so this difference is a measure of the error in our experimental results.

When the *S* field is resonantly tuned, i.e., $\Delta_S = 0$, the AT doublets seen in the excitation spectra from levels *e* and *f* appear very similar; in each case the two components have about the same intensity. When the *S* field is detuned away from the resonance the intensity ratio of the two components of the AT doublet varies differently for the fluorescence from levels *e* and *f*. Whereas the two peaks maintain approximately equal sizes for all *S*-field detunings in the *f*-level spectra, they show pronounced changes of relative sizes in the *e*-level spectra. Specifically, the peak associated with excitation of the Φ_1 component (at $\Delta_P < 0$) is stronger for $\Delta_S < 0$, while for $\Delta_S > 0$ the stronger peak is associated with the Φ_2 component (at $\Delta_P > 0$). The smaller of these peaks essentially vanishes for $|\Delta_S| \geqslant 200$ MHz.

C. Intermediate *P* field and strong *S* field

When the intensity of the *P*-laser field is increased the qualitative appearance of the spectra from levels *f* and *e* changes, as seen in Fig. 4. This figure shows spectra taken with a *P*-laser power of 2.4 mW, corresponding to a Rabi frequency of 25 MHz, and *S*-field power of 590 mW. Although the *P*-field power is here greater than the saturation power, the *P*-field Rabi frequency is substantially smaller

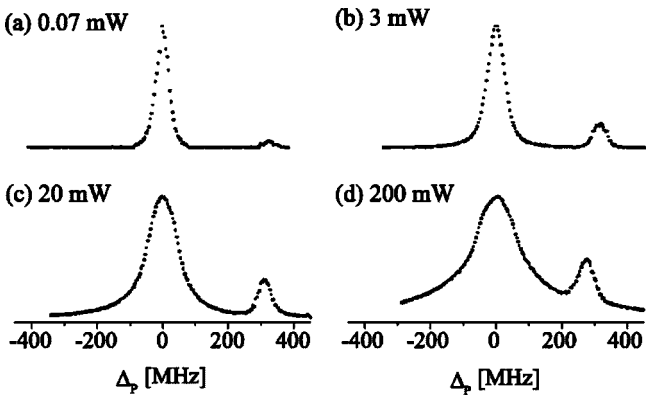

FIG. 5. Fluorescence signal of level *e* as a function of the *P*-field detuning for *P*-field power of (a) 0.07, (b) 3, (c) 20, and (d) 200 mW, corresponding to Rabi frequencies of (a) 4.2, (b) 28, (c) 71, and (d) 225 MHz. The *S*-laser detuning was −290 MHz and its power was 600 mW.

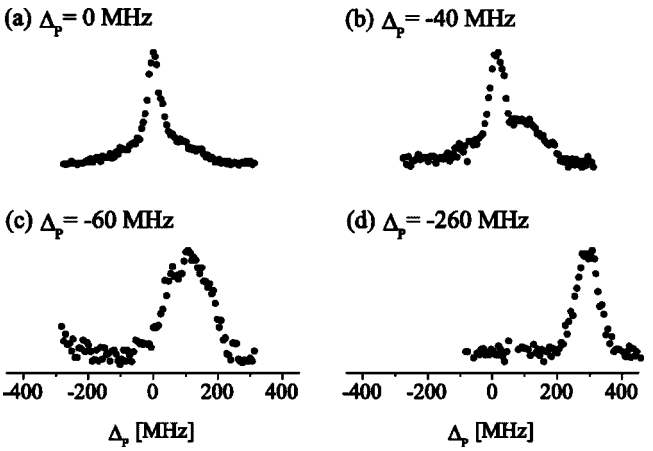

FIG. 6. Fluorescence signal from level *f* as a function of the *S*-field detuning Δ_S from resonance with the *e*-*f* transition, for four values of the detuning Δ_P of the *P* field from resonance with the *g*-*e* transition between 0 and −260 MHz. The *S*- and *P*-laser powers are 0.35 and 340 mW, respectively; the *P*-field Rabi frequency is 293 MHz.

than that of the *S* field. From the measured splittings we deduce values of the Rabi frequency Ω_S of 115±6 and 126±6 MHz, from the *f* and *e* spectra, respectively. These are in good agreement with the values of 101 and 111 MHz expected from the data of Fig. 3 with the increased *S*-field power; the differences indicate the size of our error, including reproducibility of the *P*- and *S*-laser profiles from one measurement day to another. From the measured Rabi frequencies the dipole moment was estimated to be about 0.2 D (including FC and HL factors).

Unlike the previous cases shown in Fig. 3, here the two peaks of the *f*-level spectra show a strong dependence on the *S*-field detuning, whereas the influence of this detuning on the *e*-level spectra is less pronounced. Whereas in Fig. 3(b) the smaller doublet component in the spectrum of level *e* essentially vanishes for $|\Delta_S| = 200$ MHz, in Fig. 4(a) both peaks remain distinctly visible for such large detunings of the *S* field.

For a *P* field of intermediate intensity, as in Fig. 4, the excitation spectra of levels *e* and *f* for fixed detuning of the *S* field are complementary: when the component associated with excitation of state Φ_2 is strongest in the *f*-level spectrum, then the component associated with Φ_1 is strongest in the *e*-level spectrum, and vice versa.

D. Strong *P* field and strong *S* field

Another interesting feature is observed in the excitation spectrum of level *e* when the *P*-field intensity is increased to achieve Rabi frequencies large compared to the natural linewidth of the *g*-*e* transition (12.78 MHz) and comparable to that of the *S* field. Figure 5 shows the excitation spectra of level *e* for fixed *S*-laser detuning of −290 MHz for four different *P*-laser intensities. These correspond to *P*-field Rabi frequencies of (a) 4.2, (b) 28, (c) 71, and (d) 225 MHz. Increase of the *P*-field intensity leads to an increase of the intensity of the Φ_2 component (right-hand peak) relative to that of the (broad) Φ_1 component. The increase of the Φ_2 signal saturates for very strong *P* field, but the width of the Φ_1 component continues to broaden.

E. Strong *P* field and weak *S* field

It is also interesting to study the excitation dynamics with the roles of *P* and *S* lasers interchanged, i.e., making the *P* field strong (a few hundreds of milliwatts) and using a weak (≤1 mW) *S*-laser field as a probe. A particularly careful alignment is needed in this case. To avoid full depletion of the *g*-level population by optical pumping, induced by the *P* field before the molecules reach the *S* field, the *P*-laser profile must be more tightly focused than the *S*-laser profile. Therefore we used the same geometry of *P*- and *S*-laser beams as in the previous cases.

Figure 6 shows excitation spectra of level *f* as a function of *S*-laser frequency for various detunings of the *P*-laser field and fixed *P* power of 340 mW (a Rabi frequency of 293 MHz). In contrast to the previous spectra, and also to the spectra measured under similar conditions in earlier experiments dealing with the AT effect in atoms [4], no doublets are seen for any detuning of the strong laser field (in this case *P*). Instead, only one narrow peak is observed. This occurs when the *P* field is resonant with the *g*-*e* transition [see Fig. 6(a)]. The peak develops a shoulder and broadens as the *P* field is detuned [see Figs. 6(b) and 6(c)]. It becomes narrow again as the detuning Δ_P is increased beyond ±200 MHz [see Fig. 6(d)]. The excitation spectrum of level *e* does not change when the weak *S*-field frequency is varied.

V. THEORY; DISCUSSION

Reliable quantitative analysis of the AT profiles, including height, width, and spectral separation of components, requires detailed modeling of all relevant molecular states, with all relevant spontaneous emission rates, and with the inclusion of magnetic sublevel degeneracy and Doppler-shift distributions. Such detailed analysis will be presented in a separate forthcoming publication [9]. Here we shall restrict ourselves to qualitative theoretical considerations based on

using the time-dependent Schrödinger equation for a single moving three-state molecule. Such a description treats exactly the effects of transit-time broadening of spectral features. In this section we present the theory and associated interpretation of the AT doublets as associated with adiabatic states. We also provide some general observations.

A. Magnetic sublevels

The use of linearly polarized *S* and *P* fields, with parallel polarizations, allows us to consider separate independent, three-state ladders, each labeled by magnetic quantum number *M*, whose quantization axis we take along the polarization direction (and along the molecular beam axis). Each ladder results from coherent excitation of independent sublevels, all with equal value of *M*, belonging to the three rotational angular momentum states J'', J', and J. This idealization is justifiable as long as we deal with an open system that has negligible coupling of separate ladders by spontaneous emission. For the system of interest, starting from angular momentum $J''=7$ there are $2J''+1=15$ separate ladders. Signals are observed from those sublevels of levels *e* and *f* for which $|M|\leqslant 7$. The present work treats these as a single three-state system. Two sorts of approximations are involved in this idealization. On the one hand, we disregard coupling of ladders by interlinked spontaneous emission. On the other hand, as just noted, the presence of independent ladders acts, as does Doppler broadening, to yield an inhomogeneously broadened AT profile: each ladder contributes, with an appropriate weight and appropriate AT shift, to the observed spectrum. The following arguments, combined, justify the neglect of sublevel broadening of the AT profiles.

(1) First, the supersonic expansion of a diatomic gas tends to preferentially populate angular momentum states having small values of $|M|$ [16].

(2) Next, in the weak-field excitation from this set of unequally populated sublevels, the excitation rates, which are proportional to the squares of Clebsch-Gordan (CG) coefficients, tend to favor excitation from states with small $|M|$ [11,17].

(3) Further, emission occurs from those excited sublevels for which $|M|\leqslant 7$. In general there are three distinct emission fields, termed σ_+, π, and σ_-, associated with $\Delta M \equiv M_f - M_e$ of $+1, 0$, and -1. These three fields have different angular distributions of intensity; in the x,y plane where our detectors lie, the σ fields are each half as intense as the π fields. Although each sublevel has the same decay rate, the relative rate of emission of a specific field is proportional to the square of a CG coefficient. The product of this emission rate with the field intensity, summed over the possible ΔM values from a sublevel, gives the probability of detecting decay from that sublevel. This probability also favors detection of emission from states with small $|M|$.

(4) Finally, the resonant AT splitting for each chain is proportional to a CG coefficient. The largest shifts occur for small $|M|$, but there is only a relatively small difference between the shifts of adjacent ladders.

When all these effects are combined, they produce a distribution of resonant AT splittings that is relatively concentrated near those of small-*M* sublevels. For large detuning the AT splitting is dominated by the detuning, and magnetic sublevels have even less influence. From these considerations we conclude that the inhomogeneous broadening of the AT profiles from the M_J dependence of the AT splitting is expected to be smaller than the Doppler width ($\approx$30 MHz) caused by the finite divergence angle of the molecular beam.

B. Adiabatic states

Consider the case of a well-resolved AT doublet, when the Rabi frequency of the *S* laser is much larger than all relaxation constants of the three coupled levels. The laser fields *S* and *P* vary relatively slowly during the interaction time with the molecules. Under such situation the rotating wave approximation [18] is valid and it is convenient to introduce the instantaneous eigenstates of the Hamiltonian in the absence of the *P* field $[\Omega_p(t)=0]$ and to neglect the consequences of spontaneous decay. Such eigenstates are sometimes termed *dressed* states, recognizing that when the radiation field is quantized, these states combine the properties of atoms and field [19]. Here we are concerned with slowly varying envelopes of classical fields, and so the term *adiabatic* states is more appropriate. The construction of adiabatic states of the strongly coupled *e*-*f* system involves the mixing angle $\theta(t)$, defined as

$$\tan 2\theta(t) = \frac{\Omega_S(t)}{\Delta_S}, \quad 0 \leqslant \theta \leqslant \frac{\pi}{2}. \tag{2}$$

The adiabatic states for the three-level ladder *g*-*e*-*f* coupled by a weak field *P* and a strong field *S* are

$$\Phi_3(t) = \psi_g, \tag{3a}$$

$$\Phi_2(t) = \psi_f \sin\theta(t) + \psi_e \cos\theta(t), \tag{3b}$$

$$\Phi_1(t) = \psi_f \cos\theta(t) - \psi_e \sin\theta(t), \tag{3c}$$

where ψ_j are the eigenstates of the molecular system (the bare states). As the detuning Δ_S changes from large positive to large negative values the mixing angle θ changes from 0 to 90°, and the composition of adiabatic states $\{\Phi_2, \Phi_1\}$ changes from $\{\psi_e, \psi_f\}$ to $\{\psi_f, -\psi_e\}$.

The energies $\hbar\lambda_i$ of these adiabatic states depend on the Rabi frequency of the *e*-*f* transition, and on the *P*- and *S*-laser detunings Δ_P and Δ_S:

$$\lambda_3 = \Delta_P, \tag{4a}$$

$$\lambda_2(t) = -\frac{1}{2}\Delta_S + \frac{1}{2}\sqrt{\Omega_S(t)^2 + \Delta_S^2}, \tag{4b}$$

$$\lambda_1(t) = -\frac{1}{2}\Delta_S - \frac{1}{2}\sqrt{\Omega_S(t)^2 + \Delta_S^2}. \tag{4c}$$

Although the composition of the adiabatic states changes with changing relative intensity of the two fields, adiabatic state $\Phi_2(t)$ always has higher adiabatic energy than state $\Phi_1(t)$.

The time dependence of the adiabatic states and eigenvalues comes from the slowly varying Gaussian envelope of the S field. In the present experiment, this variation is small during the relevant time interval, since the waist of the P-laser beam on the molecular beam axis is much narrower than that of the S beam. Under such conditions the S-field Rabi frequency, the concomitant mixing angle, and the adiabatic eigenvalues can be considered to be constant during the interaction with the P field: $\Omega_S(t)=\Omega_S$ and $\theta(t)=\theta$.

Spontaneous emission causes transfer of population among magnetic sublevels, an effect that cannot be treated exactly without enlarging the theory from that of a state vector, as assumed here, to that of a density matrix. However, by assuming that all spontaneous emission proceeds to final states that are not part of the three-level manifold of coherently coupled states, it is possible to treat the system as one in which spontaneous emission serves only as a loss, removing population at rates given by the inverses of radiative lifetimes (i.e., we treat the system as an open one).

Due to spontaneous emission decay the adiabatic states $\Phi_1(t)$ and $\Phi_2(t)$ are also decaying, at rates that depend on the mixing angle θ. The explicit evaluation of the transformation of the two bare-state losses γ_e and γ_f into two adiabatic-state losses Γ_2 and Γ_1 leads to the formulas [19]

$$\Gamma_2 = \gamma_e \cos^2\theta + \gamma_f \sin^2\theta, \tag{5a}$$

$$\Gamma_1 = \gamma_e \sin^2\theta + \gamma_f \cos^2\theta. \tag{5b}$$

C. Resonances

The adiabatic-state picture allows a simple interpretation of the AT effect. When the energy eigenvalue of state Φ_3 coincides with that of either Φ_2 or Φ_1, as occurs [see Eqs. (4a)–(4c)] when the detuning Δ_P is chosen to satisfy the resonance condition $\Delta_P=\lambda_j$ for $j=1,2$, then there occurs a P-field-induced transition between the ground state and the adiabatic state Φ_j. Note that because $\lambda_2>\lambda_1$, resonance with Φ_2 occurs for larger Δ_P than resonance with Φ_1, i.e., the Φ_2 peak appears at the right in our plots. Population leaves the ground state through resonance excitation of the decaying state Φ_j (optical pumping). Thus a scan of the P-field detuning will reveal, through fluorescence, two components of the AT doublet, corresponding to excitation of the two adiabatic states $\Phi_1(t)$ and $\Phi_2(t)$ followed by spontaneous emission loss.

When Δ_S is large and positive ($\theta\approx 0$), the resonance with state $\Phi_2(t)$ (which is here predominantly level e) occurs for $\Delta_P\approx 0$, while resonance with state $\Phi_1(t)$ (predominantly level f) occurs for $\Delta_P\approx -\Delta_S$. For large negative Δ_S (so $\theta\approx\pi/2$) the resonance at $\Delta_P\approx 0$ is associated with state $\Phi_1(t)$ (which is here predominantly level e).

When Δ_S is zero, the separation between the two peaks, $\lambda_2-\lambda_1$, is the Rabi frequency Ω_S. Thus the minimum separation of the doublet peaks, as a function of Δ_S, provides a measure of this Rabi frequency.

D. Evaluation of signals

For an open system it can be shown [9] that when the P field is not too strong (i.e., such that $\Omega_P<\Gamma_1,\Gamma_2$) and of sufficiently long duration (such that $1/T_P\ll\Gamma_i$) the adiabatic-state populations $N_i(t)\equiv|\langle\Phi_i(t)|\Psi(t)\rangle|^2$ are

$$N_i(t) = \frac{r_i(t)}{\Gamma_i}\exp\left[-\int_{-\infty}^{t} dt' r_i(t')\right], \quad i=1,2, \tag{6}$$

where the optical pumping rate $r_i(t)$ is given by the expression

$$r_i(t) = \frac{\Gamma_i}{4}\frac{\Omega_i^2}{\Delta_i^2+\Gamma_i^2/4}. \tag{7}$$

Here $\Delta_i=\lambda_i-\lambda_3$ is the effective detuning of the P field from resonance with the adiabatic state Φ_i and Ω_i is the effective Rabi frequency for the transition $\Phi_3(t)\rightarrow\Phi_i(t)$:

$$\Omega_2(t) = \Omega_P(t)\cos\theta, \quad \Omega_1(t) = \Omega_P(t)\sin\theta. \tag{8}$$

The populations $P_n(t)\equiv|\langle\psi_n|\Psi(t)\rangle|^2$ of the bare states can be expressed in terms of the adiabatic-state populations as

$$P_e(t) = N_2(t)\cos^2\theta + N_1(t)\sin^2\theta, \tag{9a}$$

$$P_f(t) = N_2(t)\sin^2\theta + N_1(t)\cos^2\theta. \tag{9b}$$

From these expressions we can obtain the fluorescence signal from level $n=e,g$ through resonance with adiabatic state $\Phi_i, i=1,2$. This signal is proportional to the relative intensity $I_n^{(i)}$ of emission from a single molecule. For example, resonance with the state Φ_1 results in fluorescence from level e with relative intensity

$$I_e^{(1)} = \gamma_e\int_{-\infty}^{+\infty} dt\ P_e(t) = \gamma_e\sin^2(\theta)\int_{-\infty}^{+\infty} N_1(t)dt$$

$$= \frac{\gamma_e\sin^2(\theta)}{\Gamma_1}[1-\exp(-R_1)], \tag{10}$$

where $R_i=\int_{-\infty}^{\infty}dt\ r_i(t)$. For a Gaussian probe pulse $\Omega_P(t)=\Omega_P(0)\exp(-t^2/T_P^2)$, where $T_P=\tau_{pulse}/\sqrt{2\ln 2}$, we have $R_1=R_1(0)\sin^2\theta$ and $R_2=R_2(0)\cos^2\theta$ where

$$R_i(0) = \frac{1}{4}\sqrt{\frac{\pi}{2}}\frac{\Gamma_i T_P\Omega_P(0)^2}{\Delta_i^2+\Gamma_i^2/4}. \tag{11}$$

The expressions for the intensities $I_f^{(1)}$, $I_e^{(2)}$, and $I_f^{(2)}$ can be obtained in a similar way.

Table I shows the relative intensities $I_n^{(i)}$ of the components of the Autler-Townes spectra for weak ($R_i\ll 1$) and saturating ($R_i\gg 1$) P fields. If the molecular beam is not sufficiently collimated these expressions have to be averaged over Doppler shifts.

E. Evaluation: Weak probe; lifetime

When the P field is weak, the intensities of the components of the AT doublet in the excitation spectrum of level f are each proportional to the same factor $\cos^2(\theta)\sin^2\theta$ (see

TABLE I. The relative single-molecule fluorescence intensities $I_n^{(i)}$ in the excitation spectra from levels e and f, for weak and saturating intensities of the P field. For each spectrum, e or f, the AT doublet components are Φ_1 or Φ_2.

Level n	Resonance i	Relative fluorescence intensity $I_n^{(i)}$	
		Weak P	Saturating P
e	Φ_1	$\frac{\gamma_e}{\Gamma_1}R_1(0)\sin^4(\theta)$	$\frac{\gamma_e}{\Gamma_1}\sin^2(\theta)$
	Φ_2	$\frac{\gamma_e}{\Gamma_2}R_2(0)\cos^4(\theta)$	$\frac{\gamma_e}{\Gamma_2}\cos^2(\theta)$
f	Φ_1	$\frac{\gamma_f}{\Gamma_1}R_1(0)\sin^2(\theta)\cos^2(\theta)$	$\frac{\gamma_f}{\Gamma_1}\cos^2(\theta)$
	Φ_2	$\frac{\gamma_f}{\Gamma_2}R_2(0)\sin^2(\theta)\cos^2(\theta)$	$\frac{\gamma_f}{\Gamma_2}\sin^2(\theta)$

Table I). This can be interpreted as a result of the interplay between different excitation rates of the adiabatic states Φ_1 and Φ_2, which are proportional to $\sin^2\theta$ and $\cos^2\theta$, respectively, and of the different contributions of the state f to these adiabatic states, which are proportional to $\cos^2\theta$ and $\sin^2\theta$, respectively. Hence the intensities of both components have almost the same dependence on the mixing angle θ; they differ only due to the different effective relaxation rates of the adiabatic states Γ_1 and Γ_2. This is experimentally observed [see Fig. 3(a)]. By contrast, the weak-P intensities of the two components in the excitation spectra of level e have very different dependence on θ, as is observed in Fig. 3(b).

From Table I and from the expression (11) for optical pumping rates we conclude that in the case of a well-collimated beam, when Doppler shifts are negligible, the ratio of the peak intensities is

$$\rho_f^{(int)} \equiv \frac{I_f^{(2)}}{I_f^{(1)}} = \left(\frac{\Gamma_1}{\Gamma_2}\right)^2 = \left(\frac{\gamma_e \sin^2\theta + \gamma_f \cos^2\theta}{\gamma_e \cos^2\theta + \gamma_f \sin^2\theta}\right)^2. \quad (12)$$

Since the mixing angle θ is known, measurement of the ratio $\rho_f^{(int)}$ of the peak intensities of the two doublet components allows the determination of the ratio of decay rates γ_e and γ_f. In molecular beam experiments the collisional damping rates are negligible. Therefore γ_e/γ_f is equal to the lifetime ratio of the two levels, τ_f/τ_e. Since in optical double-resonance schemes the lifetime of the intermediate level e is usually known, the lifetime of the upper level f can be obtained. Note that for large *positive* detunings Δ_S, $\sin^2\theta \to 0$, and Eq. (12) reduces to $\rho_f^{(int)} = (\gamma_f/\gamma_e)^2$. For large *negative* detunings $\cos^2\theta \to 0$, and Eq. (12) becomes $\rho_f^{(int)} = (\gamma_e/\gamma_f)^2$.

When the molecular beam is not ideally collimated, so that the Doppler width exceeds the lifetime width γ_e, as is the case for the present experiments, the distribution of molecular velocities contributes inhomogeneous broadening to the observed AT profiles and their interpretation is more complicated. In this case the ratio of peak intensities $\rho_f^{(int)}$ depends on the peak widths, and therefore it is better to consider the peak area ratio in the AT spectra of the upper level f, which reads

$$\rho_f^{(area)} \equiv \frac{\int d\Delta_P I_f^{(2)}(\Delta_P)}{\int d\Delta_P I_f^{(1)}(\Delta_P)} = \frac{\Gamma_1}{\Gamma_2} = \frac{\gamma_e \sin^2\theta + \gamma_f \cos^2\theta}{\gamma_e \cos^2\theta + \gamma_f \sin^2\theta} \quad (13)$$

for arbitrary Doppler width.

We have used a series of measurements of the ratio $\rho_f^{(area)}$ with different detunings (i.e., different θ values) and a fixed $\gamma_e = 1/\tau_e$ to find the γ_f that provides the best fit to Eq. (13). Using this procedure we determine the lifetime of level f to be $\tau_f = 1/\gamma_f = 17 \pm 3$ ns.

We have assumed that spontaneous emission can be treated simply as a loss of population. In reality, however, one deals with systems of levels, each of which consists of magnetic and/or hyperfine sublevels, wherein some fraction of the population of level f decays back to the level e. Therefore, a more complete analysis based on the solution of density matrix equations is needed. Nevertheless, the analysis presented here is qualitatively correct. A detailed analysis [9] shows that it is still possible to use the approach presented here for the determination of excited-state lifetimes from the ratios of doublet component areas in the AT spectrum of level f, although the formulas are more complicated than Eqs. (12) and (13).

F. Evaluation: Strong probe; branching

We have commented in Sec. IV C on the interpretation of the data displayed in Fig. 4; the relative peak heights are explained by referring to the last column of Table I. Further useful information can be gained by considering the excitation spectrum of the e level for strong P-field intensity and large detuning Δ_S (see Fig. 5). We interpret these spectra, taken for large negative detuning, as follows. Component Φ_1 (the left-hand peak) is associated with the one-photon resonance of the P-laser frequency with the g-e transition, which broadens with increasing P-field intensity. Component Φ_2 (the right-hand peak) corresponds to the two-photon resonance with the g-f transition involving one P photon and one S photon. This transition is seen in the excitation spectrum of level e because part of the f-level population spontaneously decays to the level e. If the P-field intensity is sufficiently strong to deplete significantly the population of level g due to optical pumping driven by the two-photon transitions then the intensity of the Φ_2 component will not increase further. The ratio of the intensities of the Φ_1 and Φ_2 components will then be equal to the fraction of the population of level f that has spontaneously returned to the level e, thus serving as a measure for the corresponding branching ratio.

In the present experiment the signal registered by detector PM2, which we have called the level-e fluorescence, actually

detects the total fluorescence from the $A\,^1\Sigma_u^+$ electronic state. Therefore, the peak ratio in Fig. 5(c) or Fig. 5(d) gives the fraction of the level f ($5\,^1\Sigma_g^+, v=10, J=9$) population that spontaneously decays into rovibronic levels of the $A\,^1\Sigma_u^+$ state. We measured this to be $r_{tot}=0.33$ with a statistical error of ±0.01. Because the signals are for saturated transitions, these measurements are not affected by the intensity fluctuations or frequency drift that affect measurements of Rabi frequencies, nor are they affected by inaccuracy of absolute intensity measurements. The remaining loss is attributed to the decay into the $2\,^1\Sigma_u^+$, $3\,^1\Sigma_u^+$, $B\,^1\Pi_u$, or $C\,^1\Pi_u$ electronic states, or to predissociation. From r_{tot} we obtain the fraction of decays that go to level e by multiplying by the appropriate Franck-Condon factor $S_{FC}=0.94$ [12] and Hönl-London factor $S_{HL}=0.47$, with the result $r_e=r_{tot}S_{FC}S_{HL}=0.145$ with a statistical error of ±0.004.

G. Effect of optical pumping

The excitation spectra of level f (see Fig. 6), obtained by exposing the g-e-f ladder to a strong P field and using a weak S field as a probe do not show the doublet pattern of other spectra. Nevertheless, these spectra can also be interpreted in terms of the adiabatic states.

The three-level system g-e-f considered here is open, as is typical for molecules. Strong coupling of the states g and e by the P field creates adiabatic states which are linear combinations of bare states g and e. An admixture of state e with state g results in optical pumping of the population out of the g-e system, due to the spontaneous decay of state e to other rovibrational levels of the ground electronic state. The closer the P field is to the g-e resonance, the faster will be the population depletion by optical pumping. Scanning a weak S-field frequency across the e-f resonance will thus show absorption from the adiabatic states only from those (upstream) parts of the P-field profile where the g-level population is not yet depleted. As a result of the interplay between the eigenvalue shift induced by the P field and the optical pumping (partial depletion) of the ground-state population the excitation spectrum of the e level will be significantly altered.

A detailed description of the spectra with strong P field and weak S field requires numerical simulations, either of the Schrödinger equation or of density matrix equations. Such an analysis will be presented in a forthcoming publication [9].

VI. CONCLUSION AND OUTLOOK

We have here reported studies of the coherent excitation dynamics in an open three-level ladder system with at least one of the couplings being sufficiently strong to result in substantial Autler-Townes splitting. We have shown that, depending on the coupling strength of the P and S lasers, characteristic and distinctly different spectral profiles result. We also show that the observed spectral features can be used for the characterization of highly excited molecular states.

The ratio of the lifetimes of the levels e and f can be determined from the peak area ratio in the AT spectra of the upper level f of the ladder using cw excitation and time-averaged detection as we describe in Sec. V E. The arrangement of an AT experiment is the same as that of standard spectroscopic double-resonance experiments [20], except that care must be taken to ensure a precise adjustment of overlap of the S- and P-laser beams. Moreover, the AT spectra from the intermediate level e, obtained with a strong P field, provide information about the branching in the decay of the excited level f, as we describe in Sec. V F.

Our results show that the spectral profiles of the Autler-Townes components in open three-level systems in molecules are significantly different from those observed in closed or approximately closed three-level systems of atoms. Such peculiarities of the AT spectra in open systems are caused by a dynamic interplay of the AT effect and optical pumping.

ACKNOWLEDGMENTS

This work was supported by the EU-FP5-RTN, Contract No. HPRN-CT-2002-309 (QUACS), Deutsche Forschungsgemeinschaft, INTAS (Contract No. 2001-155), and through the Max-Planck-Forschungspreis (K.B.). We thank M. Lyyra and M. Auzinsh for helpful discussions, and L. Meyer for assistance with the laser operations.

[1] W. Demtröder, *Laser Spectroscopy* (Springer, Berlin, 2003).

[2] S. H. Autler and C. H. Townes, Phys. Rev. **100**, 703 (1955).

[3] A. M. Bonch-Bruevich and V. A. Khodovoi, Sov. Phys. Usp. **10**, 637 (1968); T. Hänsch, R. Keil, A. Schabert, C. Schmelzer, and P. Toschek, Z. Phys. **226**, 293 (1969).

[4] A. M. Bonch-Bruevich, N. N. Kostin, V. A. Khodovoi, and V. V. Khromov, Sov. Phys. JETP **29**, 82 (1968); C. Delsart and J. C. Keller, J. Phys. B **9**, 2769 (1976); J. L. Picque and J. Pinard, *ibid.* **9**, L77 (1976); H. R. Gray and C. R. Stroud, Jr., Opt. Commun. **25**, 359 (1978); P. T. H. Fisk, H. A. Bachor, and R. J. Sandeman, Phys. Rev. A **33**, 2418 (1986); **33**, 2424 (1986); **34**, 4762 (1986); B. K. Teo, D. Feldbaum, T. Cubel, J. R. Guest, P. R. Berman, and G. Raithel, *ibid.* **68**, 053407 (2003).

[5] J. A. Beswick, C. R. Seances Acad. Sci., Ser. B **270**, 245 (1970); C. Cohen-Tannoudji and S. Reynaud, J. Phys. B **10**, 345 (1977); W. A. McClean and S. Swain, *ibid.* **10**, 143 (1977); R. M. Whitley and C. R. Stroud, Jr., Phys. Rev. A **14**, 1498 (1976); J. P. D. Martin, *ibid.* **57**, 2002 (1998); M. Bosticky, Z. Ficek, and B. J. Dalton, *ibid.* **57**, 3869 (1998); F. C. Spano, J. Chem. Phys. **114**, 276 (2001).

[6] B. Girard, G. O. Sitz, R. N. Zare, N. Billy, and J. Vigue, J. Chem. Phys. **97**, 26 (1992); A. F. Linskens, N. Dam, J. Reuss, and B. Sartakov, *ibid.* **101**, 9384 (1994); J. Qi, G. Lazarov, X. Wang, L. Li, L. M. Narducci, A. M. Lyyra, and F. C. Spano, Phys. Rev. Lett. **83**, 288 (1999); P. Yi, M. Song, Y. Liu, R. W.

Field, L. Li, and A. M. Lyyra, Opt. Commun. **233**, 131 (2004).
[7] P. L. Knight and P. W. Milonni, Phys. Rep. **66**, 21 (1980); K. Bergmann and B. W. Shore, in *Molecular Dynamics and Spectroscopy by Stimulated Emission Pumping*, edited by H. C. Dai and R. W. Field (World Scientific, Singapore, 1995), Chap. 9.
[8] M. A. Quesada, A. M. F. Lau, D. H. Parker, and D. W. Chandler, Phys. Rev. A **36**, 4107 (1987); A. M. F. Lau and W. M. Huo, Chem. Phys. Lett. **157**, 108 (1989).
[9] R. Garcia-Fernandez, L. Yatsenko, A. Ekers, J. Klavins, B. W. Shore, N. Bezuglov, M. Auzinsh, and K. Bergmann (unpublished).
[10] G. Baumgartner, H. Kornmeier, and W. Preuss, Chem. Phys. Lett. **107**, 13 (1984).
[11] M. Auzinsh and R. Ferber, *Optical Polarization of Molecules* (Cambridge University Press, Cambridge, U.K., 1995).
[12] K. Miculis and W. Meyer (private communication).
[13] E. A. Korsunsky, W. Maichen, and L. Windholz, Phys. Rev. A **56**, 3908 (1997).
[14] I. Schmidt, Thesis, Fachbereich Chemie, Universität Kaiserslautern, 1987.
[15] M. Kulz, M. Keil, A. Kortyna, B. Schellhaa, J. Hauck, K. Bergmann, W. Meyer, and D. Weyh, Phys. Rev. A **53**, 3324 (1996).
[16] U. Hefter, G. Ziegler, A. Mattheus, A. Fischer, and K. Bergmann, J. Chem. Phys. **85**, 286 (1986).
[17] R. N. Zare, *Angular Momentum: Understanding Spatial Aspects in Chemistry and Physics* (Wiley, New York, 1988).
[18] B. W. Shore, *The Theory of Coherent Atomic Excitation* (Wiley, New York, 1990).
[19] P. R. Berman and R. Salomaa, Phys. Rev. A **25**, 2667 (1982); J. Dalibard and C. Cohen-Tannoudji, J. Opt. Soc. Am. B **2**, 1707 (1985).
[20] L. Li and R. W. Field, J. Phys. Chem. **87**, 3020 (1983); C.-C. Tsai, J. T. Bahns, and W. C. Stwalley, J. Chem. Phys. **100**, 786 (1994).